

9727
NACA TN 3442 1216

TECH LIBRARY KAFB, NM
0066596

NATIONAL ADVISORY COMMITTEE FOR AERONAUTICS

TECHNICAL NOTE 3442

A PRELIMINARY INVESTIGATION OF AERODYNAMIC
CHARACTERISTICS OF SMALL INCLINED AIR
OUTLETS AT TRANSONIC MACH NUMBERS

By Paul E. Dewey

Langley Aeronautical Laboratory
Langley Field, Va.



Washington

May 1955

ARM C
TECHNICAL LIBRARY
AFL 2811



0066596

NATIONAL ADVISORY COMMITTEE FOR AERONAUTICS

TECHNICAL NOTE 3442

A PRELIMINARY INVESTIGATION OF AERODYNAMIC
CHARACTERISTICS OF SMALL INCLINED AIR
OUTLETS AT TRANSONIC MACH NUMBERS¹

By Paul E. Dewey

SUMMARY

The aerodynamic characteristics of several outlets with inclined or curved axes discharging air into a transonic stream have been investigated. The data presented herein show the discharge coefficient of such outlets and the static-pressure distribution in the vicinity of the outlets for several values of stream Mach number and discharge flow parameter. Tuft observations, showing the vortex formations caused by the outlet discharge from a perpendicular and an inclined outlet, are also presented.

INTRODUCTION

The high auxiliary-air-flow requirements of high-speed aircraft place increased emphasis on the design of efficient outlets through which this air is returned to the outside stream. The use of small outlets to establish desired pressure fields in certain areas also finds application in boundary-layer control and in aircraft control systems. At present, very few data on outlets discharging into high-speed air-streams are available. This report, which is mainly concerned with the effects of outlet configuration and stream velocity on the discharge rate, presents some preliminary data obtained in recent tests at transonic stream Mach numbers.

Data obtained with several outlet configurations where the outlet air was discharged perpendicularly into a transonic stream were presented in reference 1. Subsequently, several inclined outlets of circular cross section have been tested in a uniform stream at Mach numbers of 0.7 to 1.3. The effects of axis inclination and curvature on the discharge coefficient and of the discharge air on the static pressure in the vicinity of the outlet are presented herein. Motion-picture studies of the vortex formation caused by the outlet discharge from both perpendicular and inclined

¹Supersedes recently declassified NACA RM L53C10, 1953.

outlets were made at low stream Mach numbers. For these tests, the pressure gradient in the vicinity of the outlet was zero when no air was discharged from the outlet.

SYMBOLS

A	cross-sectional area of outlet
D	outlet diameter
K	outlet discharge coefficient (general), $\frac{\text{Measured mass flow}}{\text{Calculated mass flow}}$
K_o	outlet discharge coefficient in still air, $\frac{\text{Measured mass flow}}{\text{Calculated mass flow}}$
M	Mach number
m	mass flow through outlet
H	local stagnation pressure
p	local static pressure
q	free-stream dynamic pressure
R	Reynolds number, based on outlet diameter
V	free-stream velocity
x	distance along wall, positive downstream
$m/\rho VA$	discharge flow parameter, $\frac{\text{Mass flow through outlet}}{\text{Stream mass flow through area equal to outlet area}}$
$\Delta p/q$	pressure coefficient, $\frac{\text{Local static pressure} - \text{Free-stream static pressure}}{\text{Free-stream dynamic pressure}}$
α	angle of inclination, measured between outlet axis and tunnel wall
ρ	free-stream mass density

APPARATUS AND PROCEDURE

Figure 1 shows the tunnel used in this investigation with one side plate removed and a cutaway outlet model mounted in the upper floor. The tunnel test section is $4\frac{1}{2}$ inches high, $6\frac{1}{4}$ inches wide, and 17 inches long.

The upper floor is a solid flat plate with an opening in which the various outlet models were mounted. The lower floor is slotted along its length so that one-fifth of its area is open. The lower side of this slotted floor opens into a chamber which partly surrounds the test section. Air was removed from this chamber through a vacuum pump. By controlling the amount of air removed through the slotted floor, any Mach number up to 1.3 can be generated in the test section.

The outlet air was supplied through a 2-inch pipe from the tunnel supply duct (fig. 2). The rate of discharge was controlled by a valve and measured with a calibrated flow nozzle installed in the pipe system. The flow rate was calculated from pressures read at a pipe tap upstream of the nozzle and a static-pressure tap in the throat of the nozzle. The outlet discharge coefficient was based upon a theoretical discharge rate determined by the stagnation pressure in the pipe upstream of the outlet and the free-stream static pressure. The stagnation temperature of the discharged air was the same as that in the free stream. To insure a uniform velocity distribution at the metering nozzle and outlet, 40-mesh screens were installed in the pipe upstream of each. The outlet stagnation pressure measured upstream of the screen has not been corrected for the loss through the screen; this leads to a maximum error on the order of 0.006 lb/sq in. which for the purpose of this investigation is considered negligible.

The form and principal dimensions of the outlets tested are shown in figure 3. All models were plastic castings with a circular cross section and $3/8$ -inch-diameter throat. Those referred to as "inclined outlets" were made with straight axes inclined at angles of 30° , 45° , and 60° to the floor of the tunnel. The "recessed curved-axis outlets" were inclined at an angle of 45° to the tunnel floor and their axes were curved to fair into a groove in the tunnel floor extending downstream from the outlet to the end of the test section. Two such models were tested, one with a recess depth of $1/8$ inch and one with a recess depth of $1/4$ inch.

Surface static pressures were read from a number of orifices along the center line of the outlet. The location of orifices close to the outlet is indicated in the cutaway model in figure 1. Slight irregularities in surface pressures caused by small imperfections in the models or misalignment in mounting did not materially affect the flow in the stream and for the purpose of this investigation are negligible. Surface

pressures were recorded photographically from a multiple-tube, mercury-filled manometer. At the same time, the data used in calculating outlet flow rates and discharge coefficients were read visually from U-tube manometers.

RESULTS AND DISCUSSION

Discharge Coefficient

Each model was calibrated to determine its discharge coefficient as a free jet discharging into still air. The discharge coefficient is the ratio of measured mass flow to the mass flow calculated from total pressure, exit pressure, and temperature. Figure 4 shows lines of constant discharge coefficient K_0 as a function of jet Reynolds number and pressure ratio. All outlets tested showed high and fairly constant discharge coefficients and a small variation with pressure ratio and Reynolds number through the range tested. The 30° inclined outlet had an extremely high discharge coefficient, ranging from 0.970 at low pressure ratios and Reynolds numbers up to 0.995 at high pressure ratios and low Reynolds numbers. The other two inclined outlets had lower coefficients; those for the 45° outlet falling between 0.935 and 0.960 and those for the 60° outlet between 0.955 and 0.970. The recessed curved-axis outlets had lower coefficients than any of the inclined outlets, as would be expected with the bend in the throat section; however, even these models showed no coefficients below 0.920.

To obtain a visual picture of the flow, metal plates coated with powdered carbon in oil were positioned to bisect the jets issuing from the inclined outlets. The resulting flow patterns are shown in figure 5. The jets from the 45° and 60° outlets are seen to be quite similar, issuing cleanly into the atmosphere. The jet from the 30° outlet, however, expands more rapidly, as part of the jet flows along the flat surface in which the outlet is mounted.

The effect of the external stream on the discharge coefficient is shown in figure 6. To facilitate comparison between various stream Mach numbers, the outlet discharge rate m has been incorporated into the dimensionless parameter $m/\rho VA$. This is the ratio of the outlet discharge rate to the rate at which air in the tunnel stream flows through a cross-sectional area equal to that of the outlet.

At the higher values of the discharge flow parameter, there is very little difference between the coefficients of the inclined outlets (fig. 6(a)). As the discharge flow parameter increases, it is to be expected that the discharge coefficients will approach their free-jet

values. Because of the general equality of the free-jet discharge coefficients, it is reasonable to expect this agreement at high discharge rates. At the lower discharge rates, the effect of inclination is seen in the spreading of the curves. Those outlets which discharge more nearly parallel to the stream have higher coefficients because of the smaller amount of interference between the outlet jet and the stream. This is true for all external stream Mach numbers. With a stream Mach number of 1.1, however, the discharge coefficients showed a much smaller spread throughout the range of discharge rates. Data from reference 1 for a 3/8-inch outlet discharging perpendicularly to the stream has been included in figure 6(a) to extend the range of inclination up to 90°.

Figure 6(b) shows the effect of the external stream on the discharge coefficients of the two recessed outlets with curved axes. The more deeply recessed outlet, with a recess depth of $\frac{2}{3} D$, has a nearly constant discharge coefficient of about 0.95 at values of $m/\rho VA$ above 0.3. As the discharge rate decreases, the coefficient rises rapidly and reaches infinity at $m/\rho VA \approx 0.15$. The reason for this is that the static pressure in the recess is below the free-stream static pressure which is used in computing the theoretical discharge rate. A recessed outlet will thus discharge air even though the internal pressure is equal to or slightly less than the free-stream static pressure. This same characteristic is seen in the outlet with a $\frac{1}{3} D$ recess depth, which has a discharge coefficient of infinity at $m/\rho VA \approx 0.09$. As the discharge rate increases, the coefficient decreases rapidly until it reaches its minimum value at $m/\rho VA \approx 0.2$ and then increases until at $m/\rho VA \approx 0.7$ it is about equal to that for the more deeply recessed outlet. The discharge coefficients for both recessed outlets appear to have reached a nearly constant value of about 0.95 for values of the discharge flow parameter above 0.7 for all stream Mach numbers. Except for the stream Mach number of 1.1 with $m/\rho VA$ below 0.7 the stream Mach number has little effect on the value of the discharge coefficient for any constant value of the discharge flow parameter.

In figure 7 the ratio of discharge coefficient to free-jet coefficient, at the same outlet Reynolds number and pressure ratio, has been plotted against discharge flow parameter for each model. This figure shows more clearly the influence of the stream velocity on the outlet discharge coefficient and compares its effect on the various outlets tested. Because the free-jet coefficients are high and nearly constant, these curves are very similar to those of figure 6. It is noted, however, that the recessed curved-axis outlets have discharge coefficients higher than their free-jet coefficients, owing to pumping by the stream, whereas the inclined outlets do not. It is to be expected that K/K_0 approaches 1.0 as an asymptote as the discharge flow parameter $m/\rho VA$ is increased.

Static-Pressure Variation

The variation of surface static pressure along a line through the center of the outlet is shown in figure 8. In order to compare the effects at various tunnel velocities, the pressure variation is presented in terms of the pressure coefficient $\Delta p/q$.

In general, the outlet discharge causes an increase in static pressure on the upstream side of the outlet and a much lower pressure on the downstream side. At subsonic stream velocities the gradient increases smoothly as the outlet is approached from upstream. At supersonic stream velocities, the pressure rises abruptly at the position of the detached shock wave upstream of the outlet. Immediately downstream of the outlet, the static pressure is far below that of the undisturbed stream. Farther downstream the pressure rises smoothly, reaching the undisturbed stream value about six outlet diameters downstream. In general, higher outlet discharge rates cause greater variations in static pressure in the vicinity of the outlet.

The static-pressure variations for the inclined outlets are presented in figures 8(a), (b), and (c). The same data for an outlet discharging perpendicularly to the stream (from ref. 1) are also presented (fig. 8(d)). The magnitude of static-pressure variations increases with the angle of inclination, the 30° outlet causing relatively small disturbances and the 90° outlet creating the greatest pressure variations.

Figures 8(e) and (f) show the static-pressure variations along the center line of the recessed curved-axis outlets. The more deeply recessed outlet shows no variation of static pressure on the upstream side, and the discharge from the less deeply recessed outlet causes only a very small increase in pressure. Because of the recess, there is a large static-pressure variation on the downstream side of the outlet with no discharge. A small outlet discharge rate brings the pressure in the recess almost to the free-stream value. This rise in pressure reaches its maximum at the value of m/pVA corresponding to the minimum value of the discharge coefficient (fig. 7(b)). As the discharge flow parameter increases above $m/pVA = 0.2$, the pressure just downstream of the outlet decreases, very much as it does for the inclined outlets. As one would expect, the pressure in the shallower recess shows more variation with flow rate than that in the deeper recess.

Vortex Formation

To obtain a better understanding of the flow disturbances resulting from the interaction of the outlet discharge and the external stream, a wool tuft on a wand was moved about slowly in the vicinity of the outlet

and a very strong vortex action was observed. Motion pictures were taken and several frames are reproduced in figure 9. For this observation, the tunnel was set up on the blower intake so that the camera could be placed in the tunnel inlet. Two outlet models were used for this study: the 30° inclined outlet, and the 3/8-inch circular thin-plate outlet of reference 1. The stream Mach number was 0.3, and the discharge flow parameter $m/\rho VA$ was about 0.95 for the inclined outlet and 0.75 for the thin plate. Figure 9 shows the disturbance in the stream caused by the outlet discharge. The slow shutter speed of the motion-picture camera causes the single-strand wool tuft to appear as a wide blur when individual frames are reproduced as still pictures. When projected as motion pictures, however, the vortices at both sides of the outlet are seen clearly. Although no data were taken to indicate the vortex strength, it was seen in the motion pictures that the vortices resulting from the discharge from the thin plate are stronger than those from the inclined outlet. This is to be expected because, at the same discharge rate, the discharge velocity component perpendicular to the stream is twice as large with the thin-plate outlet as it is with the 30° inclined outlet.

CONCLUSIONS

From this investigation of the transonic aerodynamic characteristics of small inclined air outlets, it is concluded that:

1. At low values of the discharge flow parameter, outlets whose axes are inclined have higher discharge coefficients than those whose axes are perpendicular to the air stream.
2. The recessed outlets tested have discharge coefficients higher than the inclined outlets owing to pumping by the stream which causes them to discharge air even though the internal pressure may be slightly below the static pressure on the undisturbed surface.
3. At a constant value of the discharge flow parameter $m/\rho VA$, the effect of stream Mach number on the discharge coefficient of outlets with inclined or curved axes is small.
4. The variation in surface pressure caused by the outlet discharge decreases as the angle of inclination decreases.

5. The jet issuing from an outlet into a moving airstream causes the formation of strong vortices at the edges of the wake.

Langley Aeronautical Laboratory,
National Advisory Committee for Aeronautics,
Langley Field, Va., March 6, 1953.

REFERENCE

1. Nelson, William J., and Dewey, Paul E.: A Transonic Investigation of the Aerodynamic Characteristics of Plate- and Bell-Type Outlets for Auxiliary Air. NACA RM L52H20, 1952.

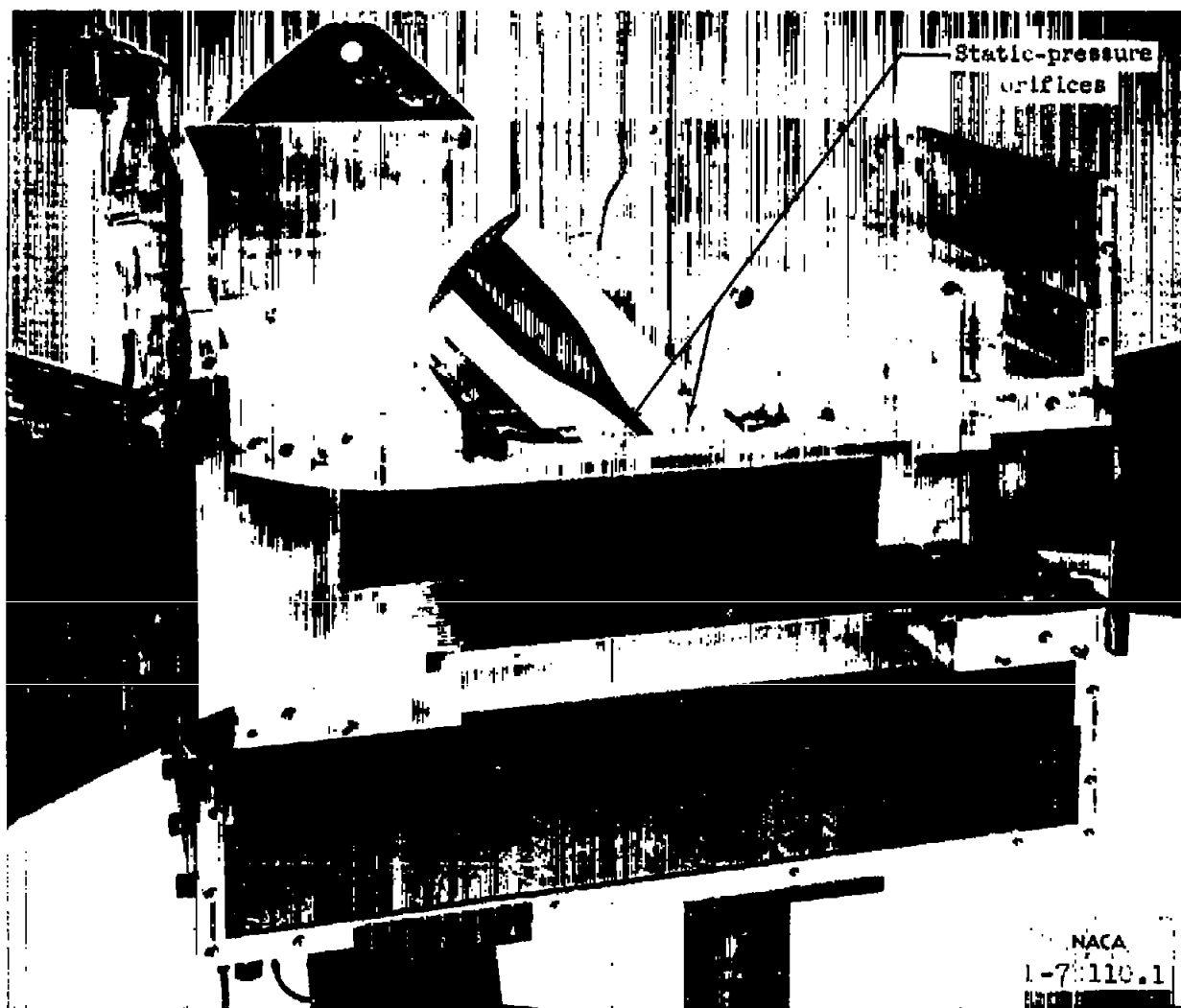


Figure 1.- Tunnel with side plate removed and cutaway outlet model mounted in upper floor.

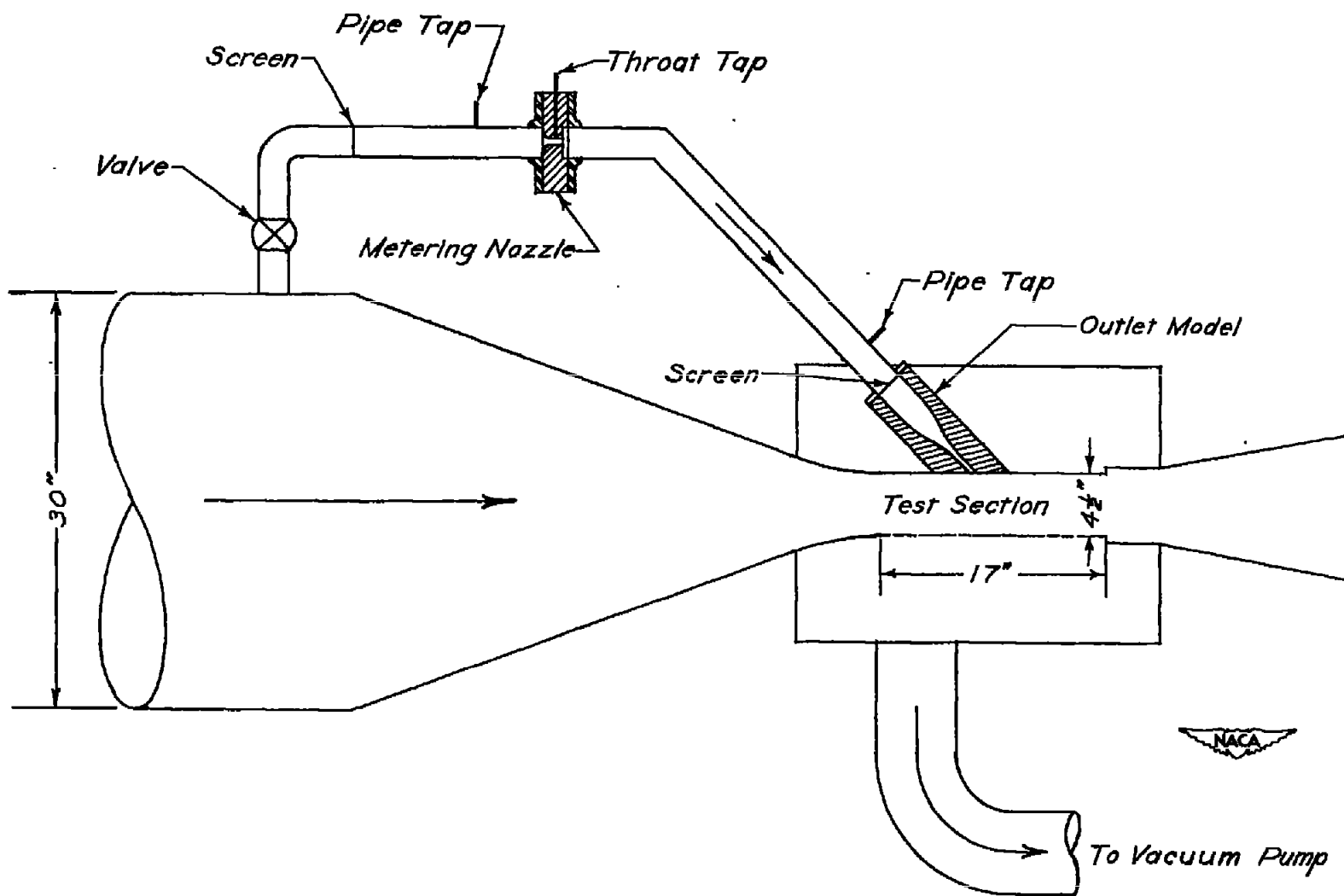


Figure 2.- General arrangement of tunnel and outlet air line.

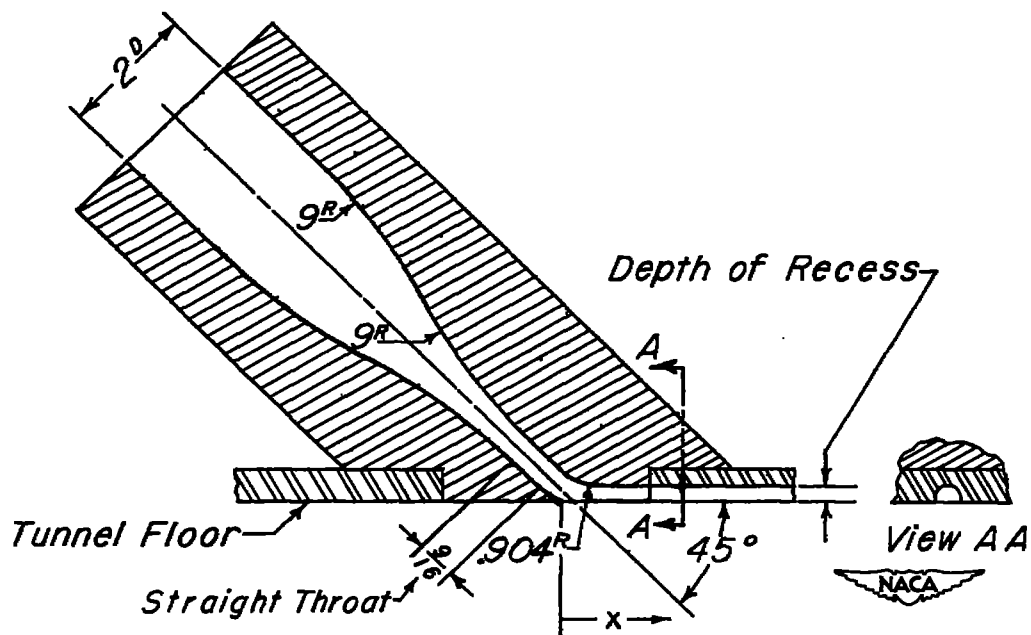
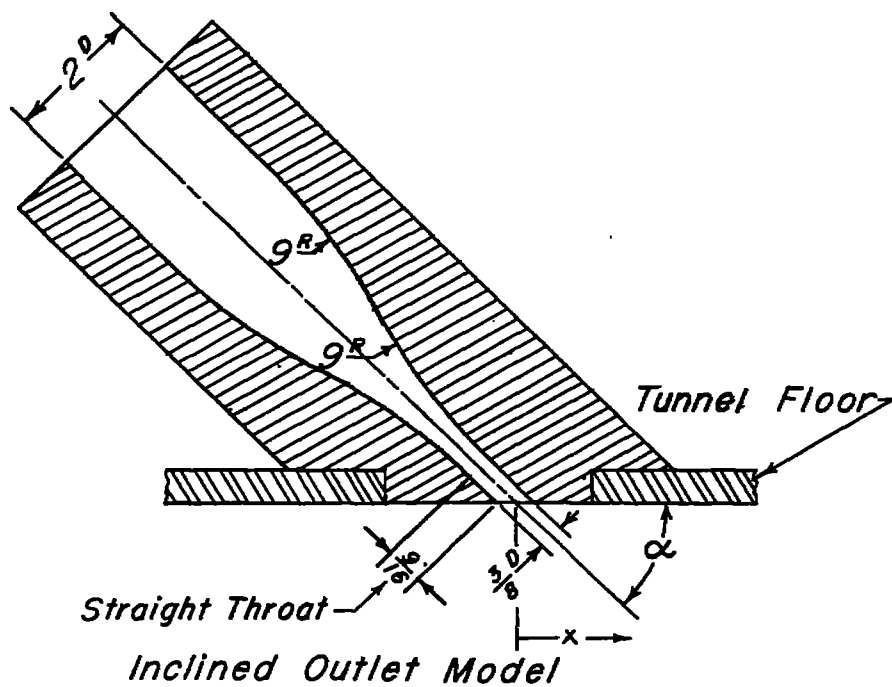


Figure 3.- Outlet models. All dimensions in inches.

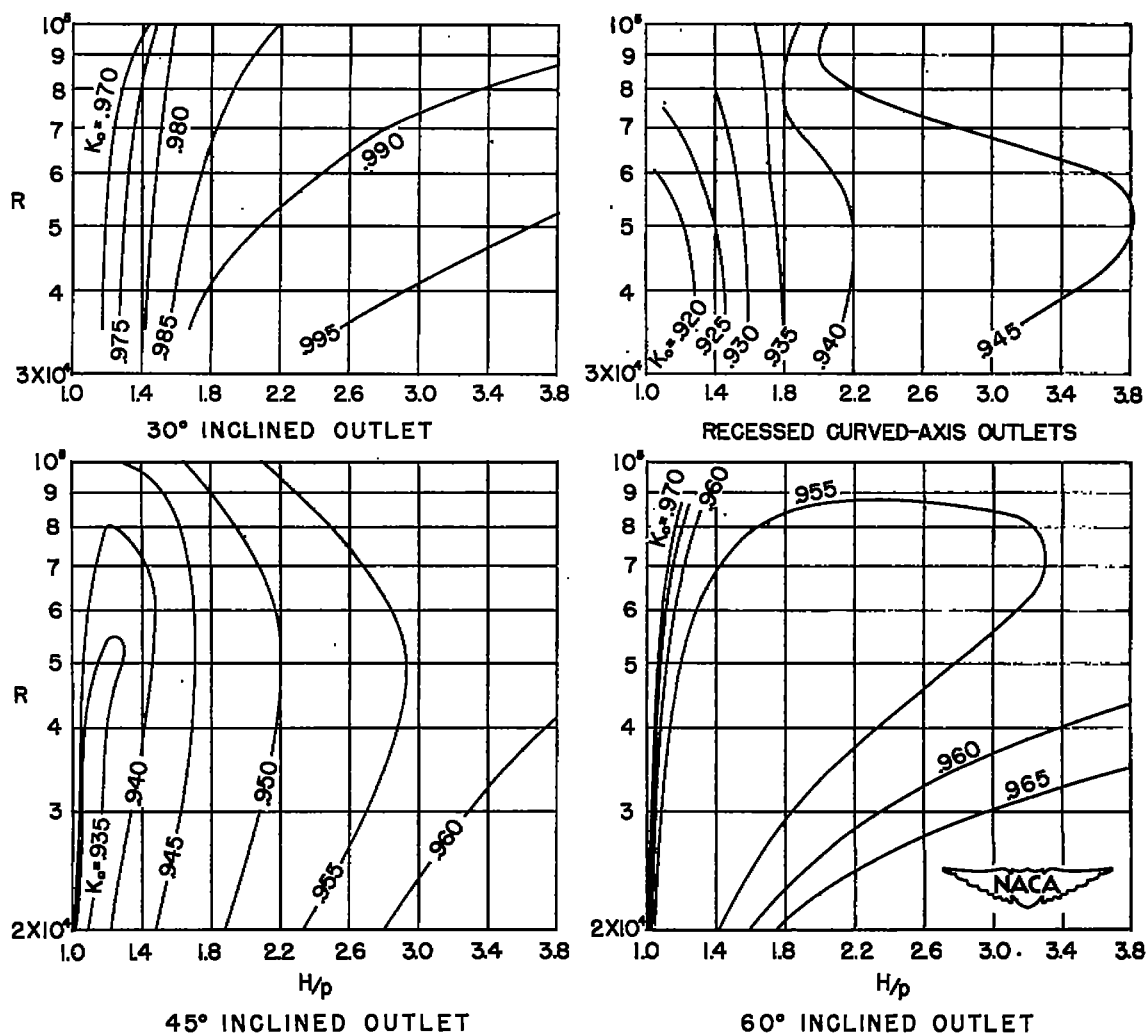
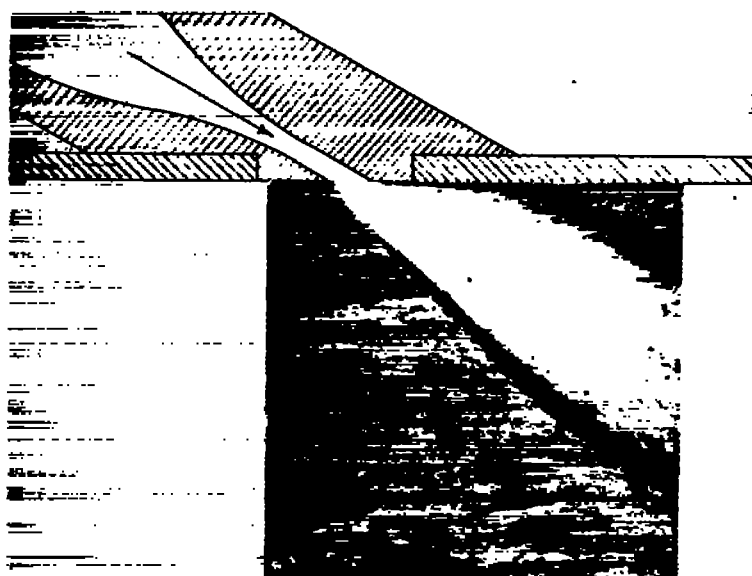
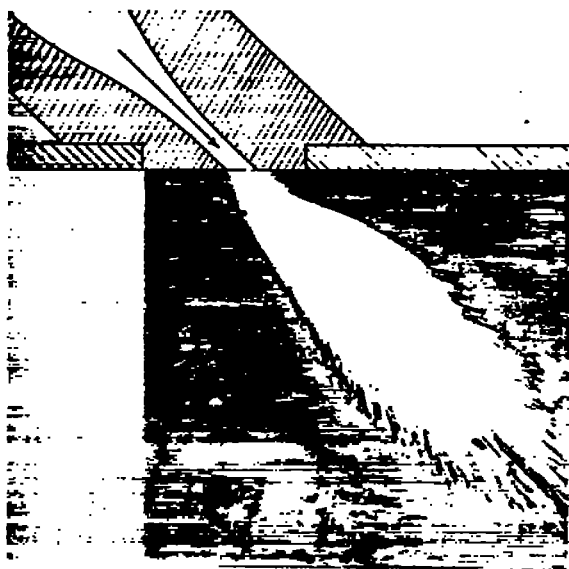


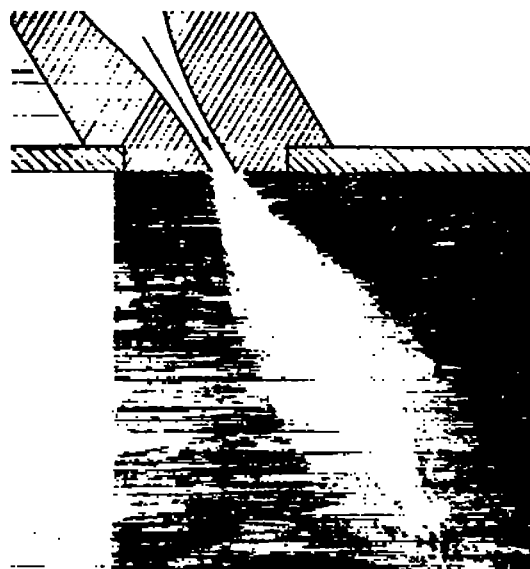
Figure 4.- Discharge coefficients for outlets as free jets discharging into still air.



30° Outlet



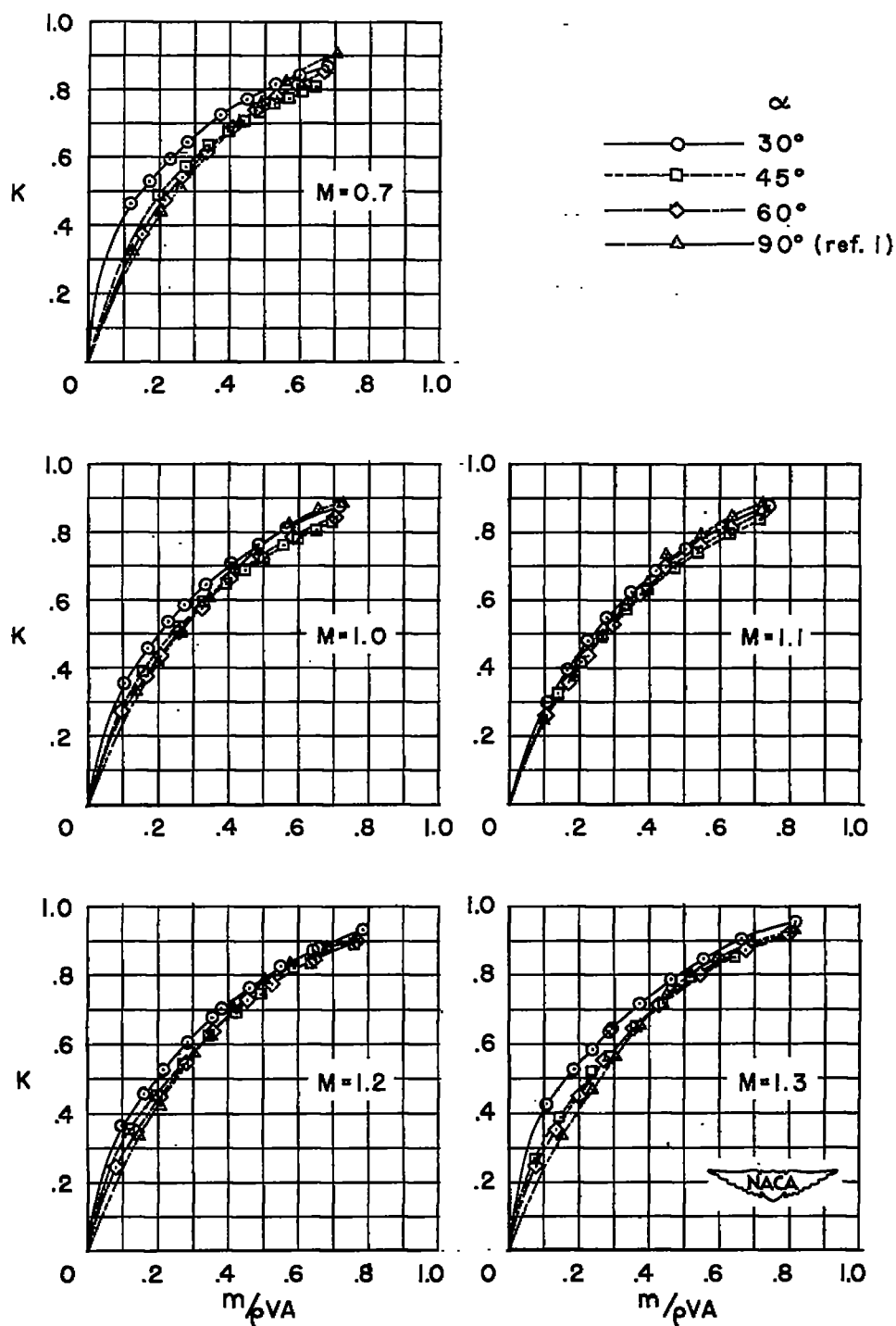
45° Outlet



60° Outlet

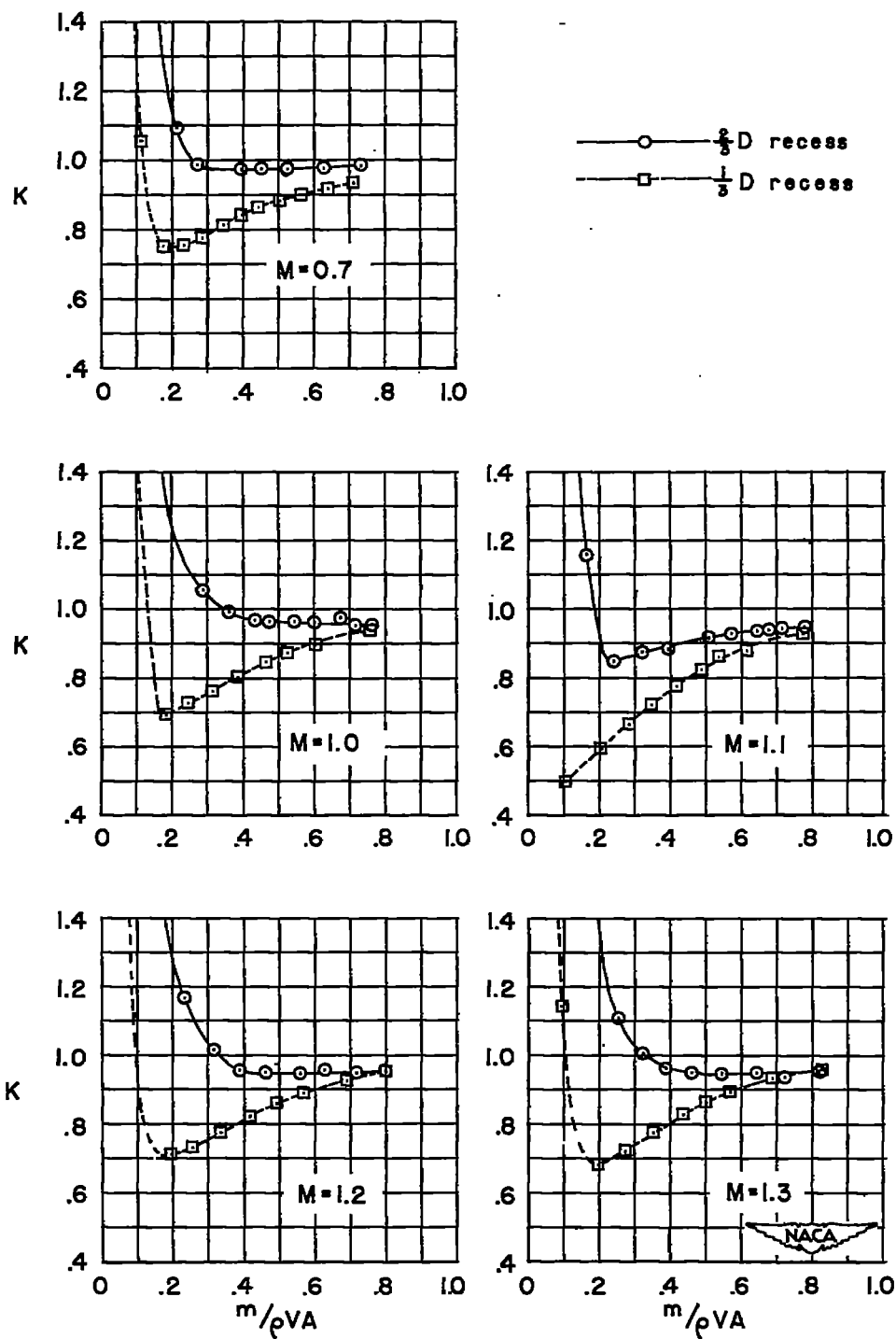
NACA
L-77959

Figure 5.- Flow patterns for inclined outlets discharging into still air.



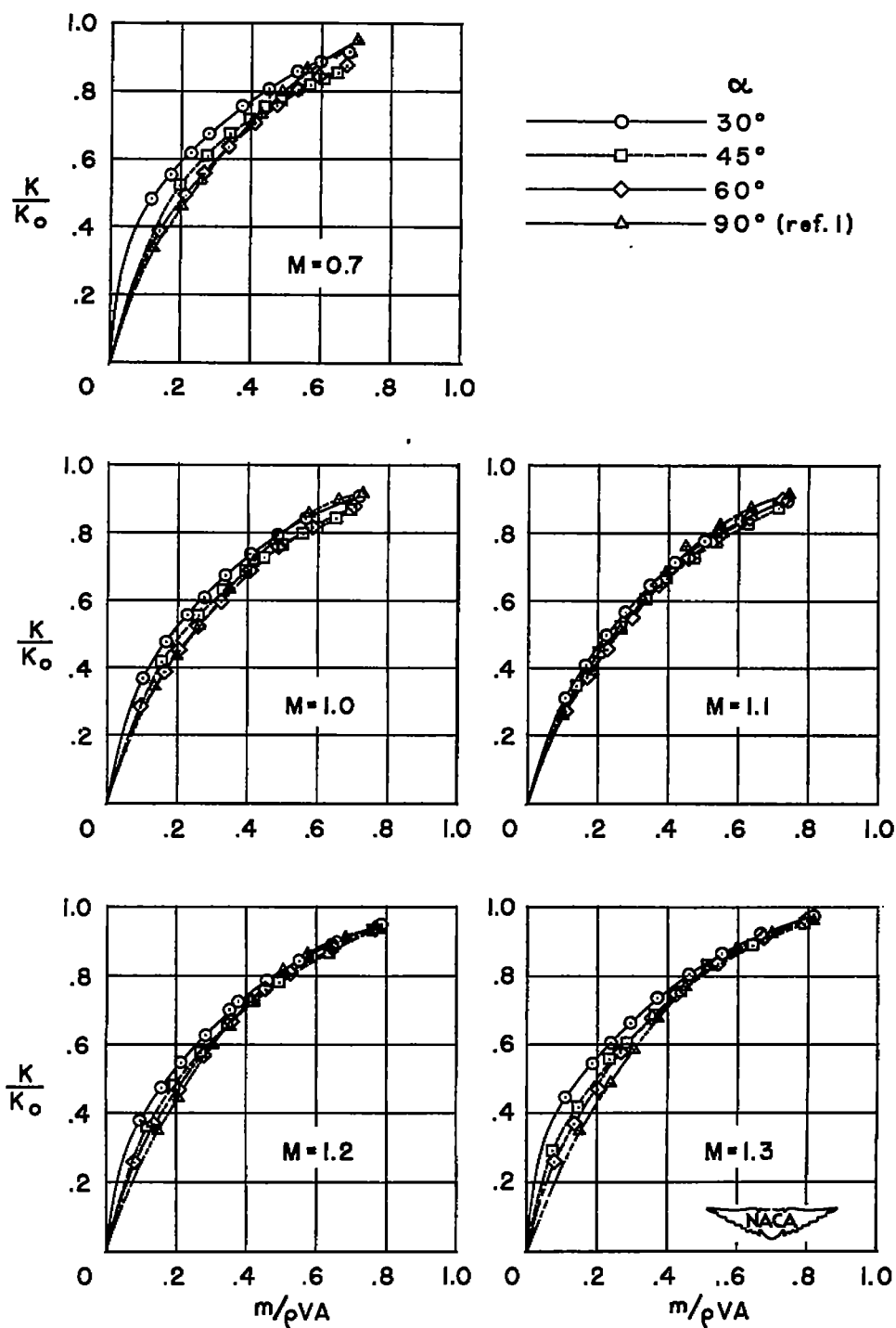
(a) Inclined outlets.

Figure 6.- Outlet discharge coefficient as a function of discharge flow parameter and stream Mach number.



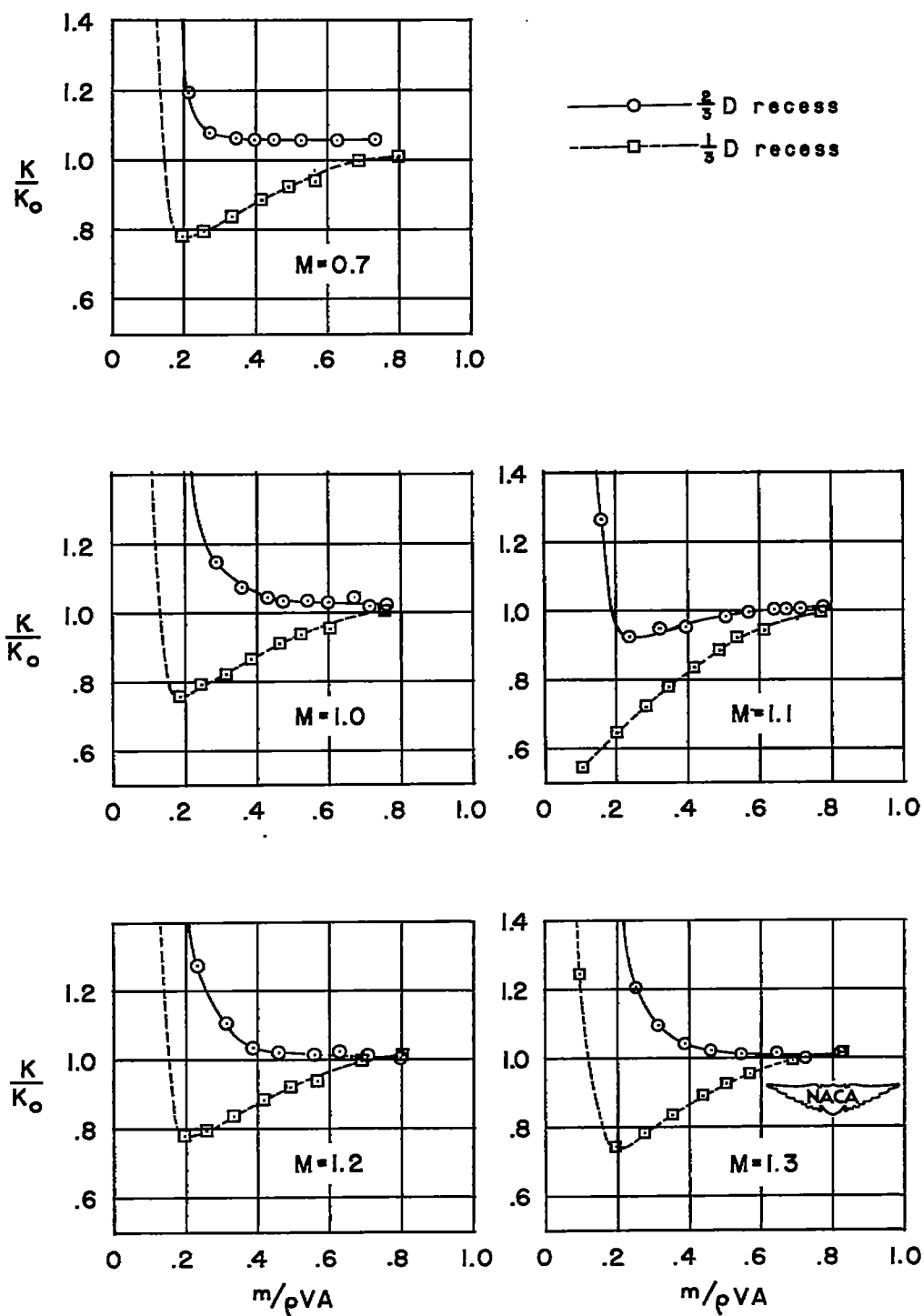
(b) Recessed curved-axis outlets.

Figure 6.- Concluded.



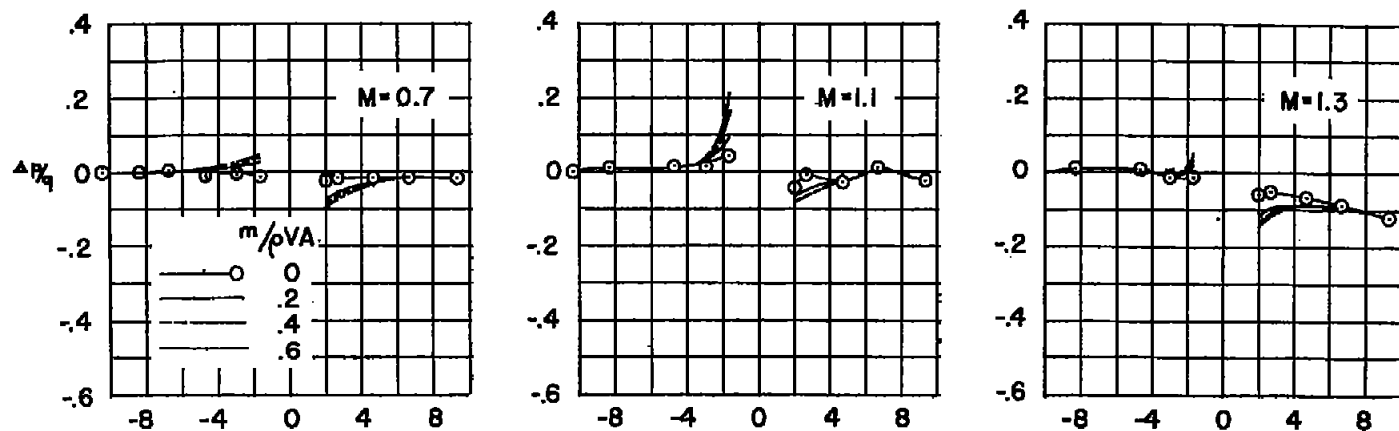
(a) Inclined outlets.

Figure 7.- Outlet discharge coefficient relative to free-jet coefficient as a function of discharge flow parameter and stream Mach number.

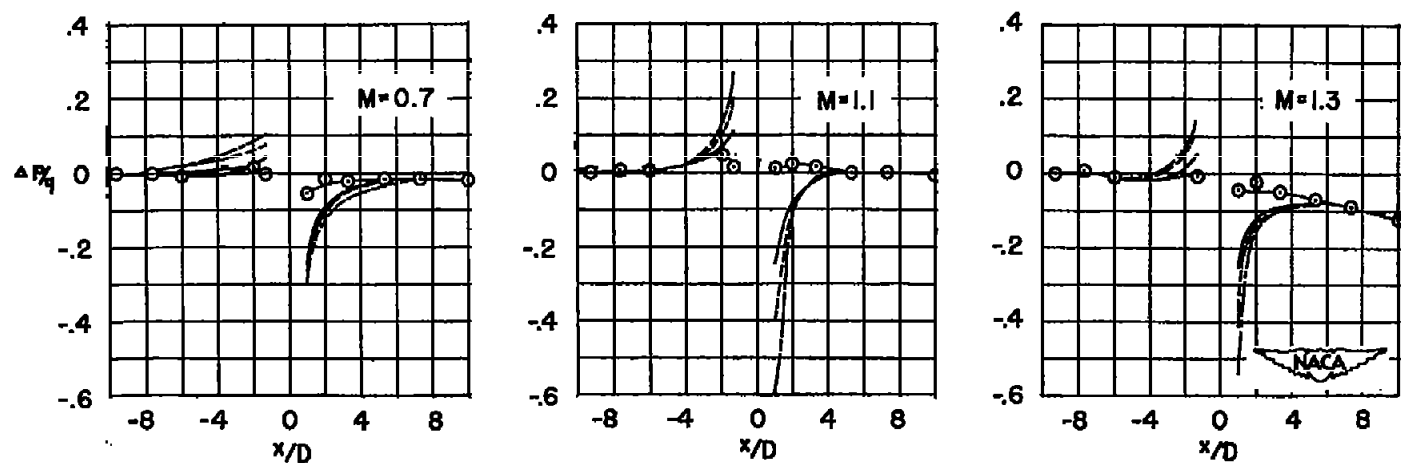


(b) Recessed curved-axis outlets.

Figure 7.- Concluded.

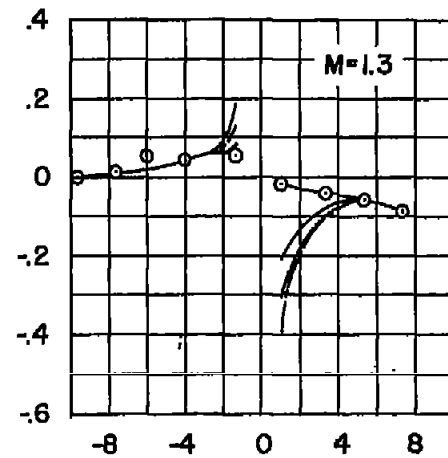
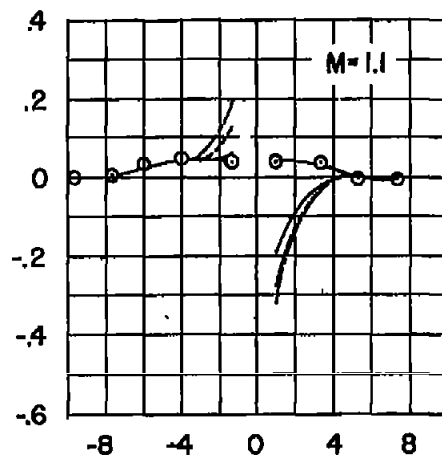
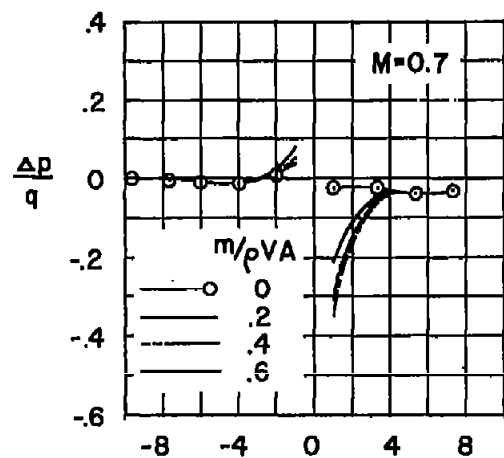


(a) 30° inclined outlet.

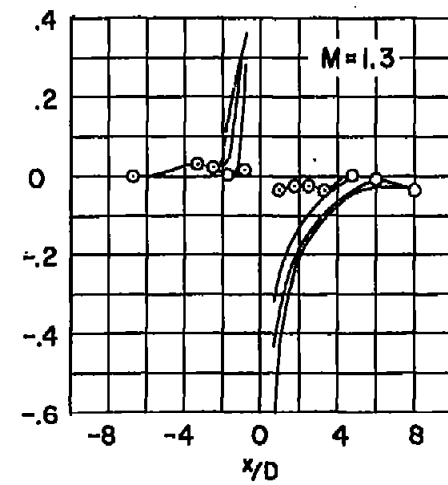
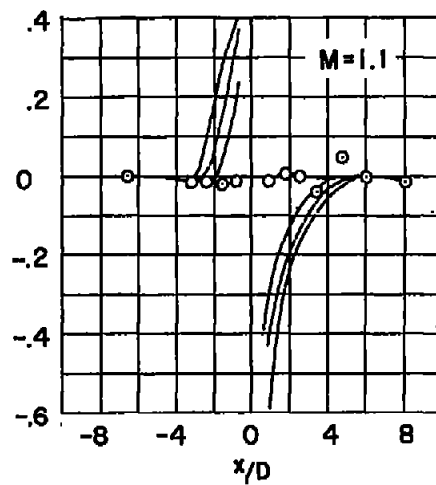
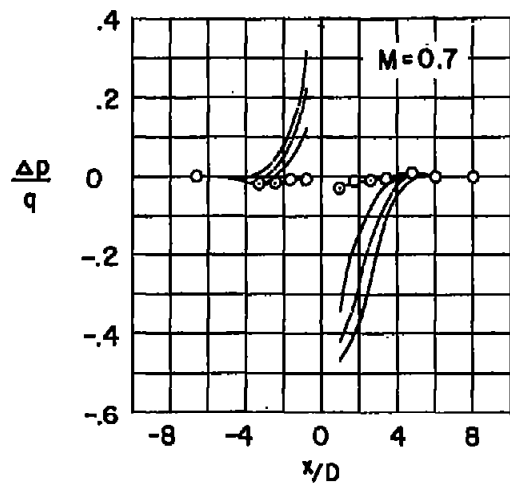


(b) 45° inclined outlet.

Figure 8.- Wall static-pressure distribution along outlet center line as a function of discharge flow parameter and stream Mach number.

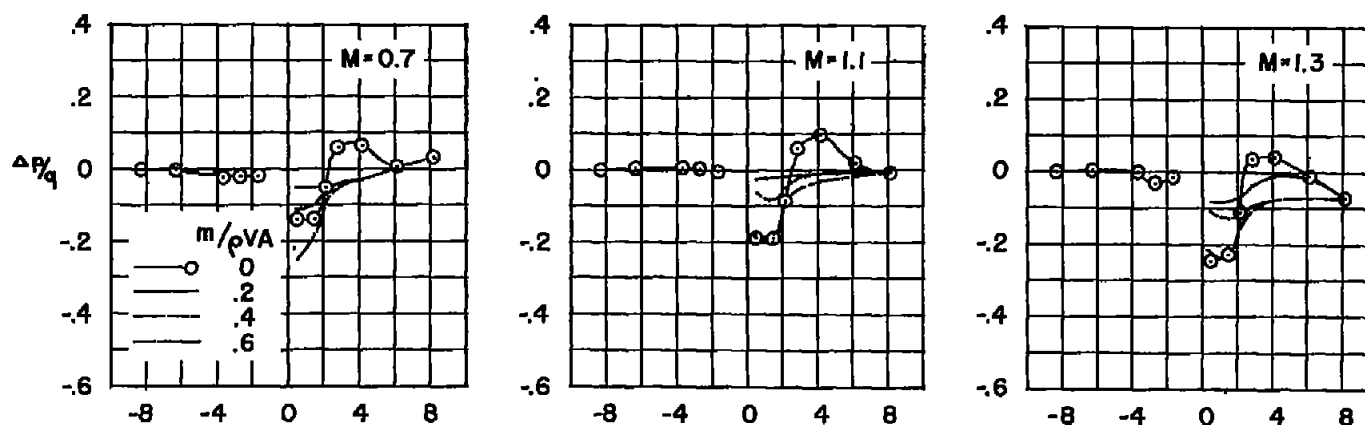


(c) 60° inclined outlet.

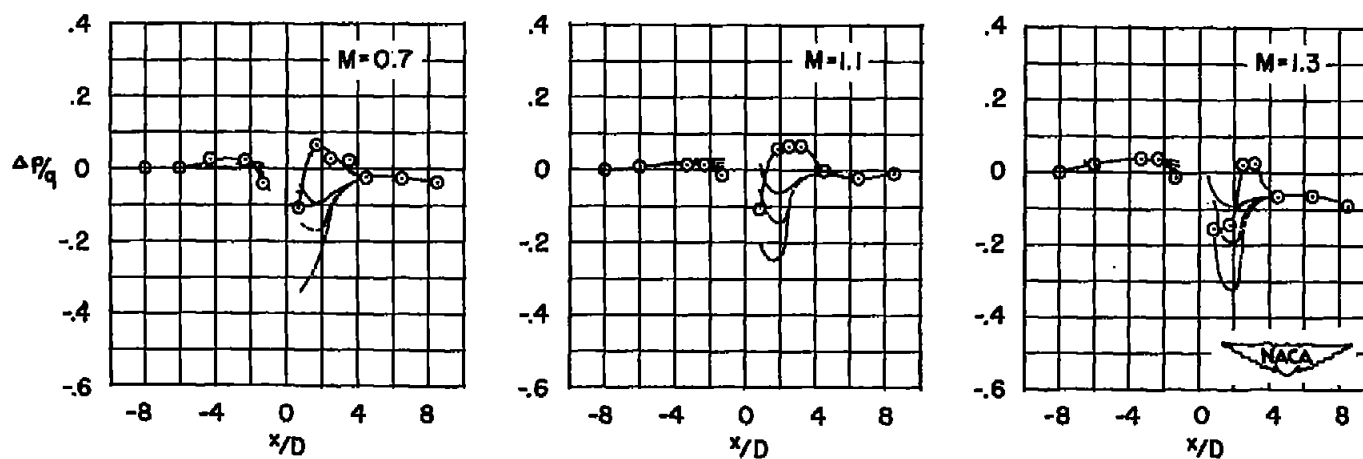


(d) 90° outlet.

Figure 8.- Continued.

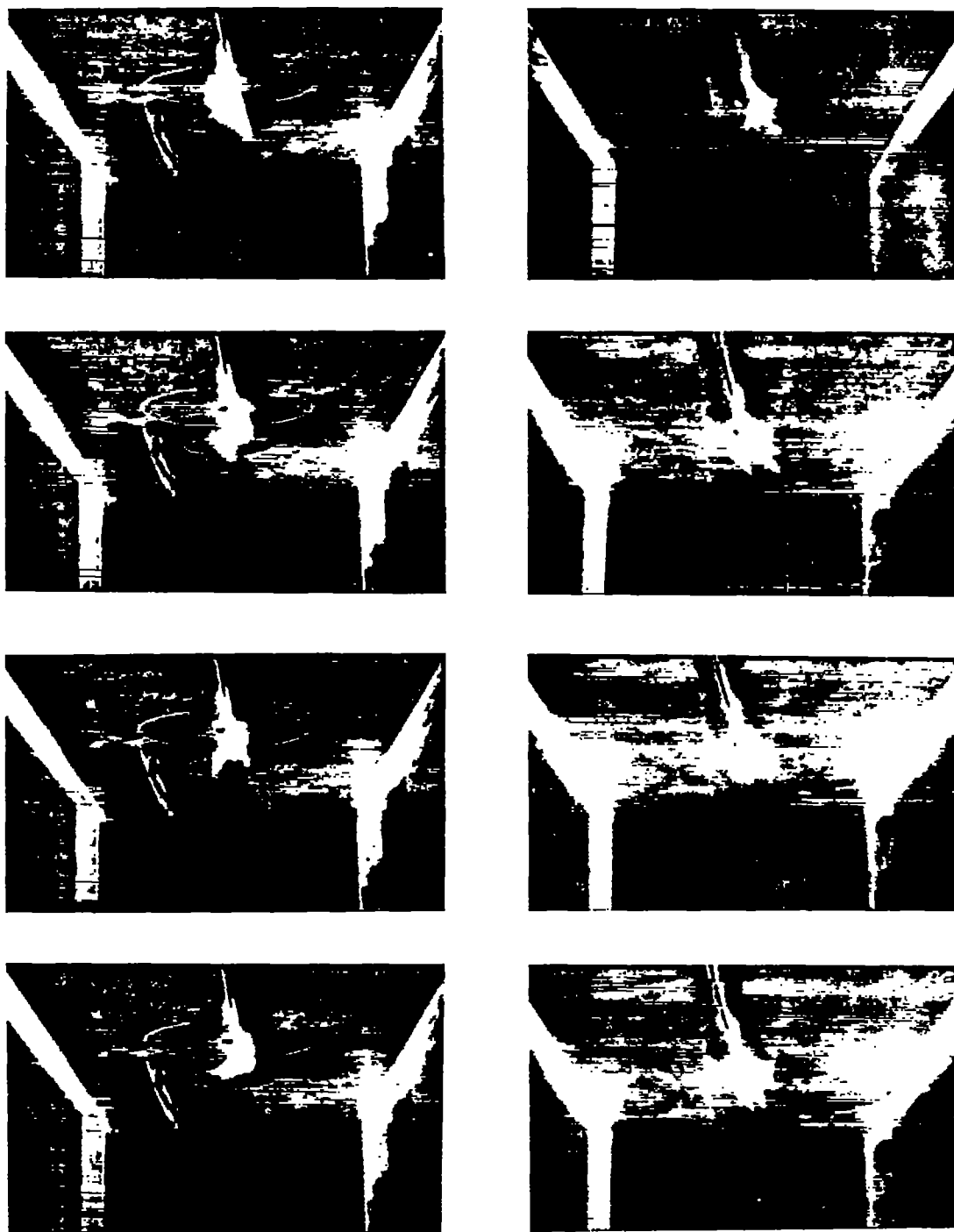


(e) $\frac{2}{3} D$ recessed curved-axis outlet.



(f) $\frac{1}{3} D$ recessed curved-axis outlet.

Figure 8.- Concluded.



(a) Thin-plate outlet (ref. 1).

(b) 30° inclined outlet.

NACA
L-77960

Figure 9.- Tuft study of vortex formation resulting from outlet discharge into a stream at a Mach number of 0.3.